Observations of the Outer Radiation Belt with REM and Comparisons with Models

E.J. Daly[1], P. Bühler[2] and M. Kruglanski[3],
[1]European Space Agency, ESTEC, 2200-AG Noordwijk, The Netherlands
[2]Paul Scherrer Institute, CH-5232 Villigen PSI, Switzerland
[3]IASB-BIRA, 3 Avenue Circulaire, B-1180 Brussels, Belgium

Abstract

Radiation Environment Monitors (REMs) on-board the *STRV-1b* spacecraft in geostationary transfer orbit (GTO) and externally on *Mir* have returned valuable results over the last few years. *STRV* data show the great variability of the electron radiation belt and a stable proton belt feature. In this paper, a detailed assessment is made of the flux values derived from the REM on *STRV* and particularly how they compare with the AE-8 and CRRESELE electron radiation-belt models. To compare with CRRESELE, the activity index Ap_{15} is used and the behavior of this index as a parameter is assessed. *GOES* data are used to aid this assessment.

I. Introduction

Two radiation environment monitors were launched in 1994. They are simple pairs of single shielded silicon diode detectors. One was placed in geostationary transfer orbit (GTO) onboard *STRV-1b* and produced data until 1998, while the second was installed externally on *Mir* in low Earth orbit and operated for two years. GTO covers the equatorial regime of inner and outer radiation belts well, while *Mir* encounters the belts near atmospheric cut-off.

Previous work [1], [2] has summarized many interesting features of the results from these experiments. The outer (electron) belt has been subject to many injection events, including the January 1997 event [3] which was the subject of special study. Correlations of the dynamics of outer zone electrons with various other solar-terrestrial parameters and seasonal flux variations have been detailed [2] and simulations of the flux "drop-outs" seen shortly before enhancements have reproduced many of the features observed [4]. Results from the proton belt observations include the existence of a possible hard proton spectral feature at the outer edge of the inner belt. *Mir* data show the strong anisotropy in the low-altitude inner (proton) belt with a clarity never seen before [5].

Current static models are inadequate for many contemporary mission and spacecraft design purposes [6]. A key requirement for developing new models is sufficient in-orbit data. Low-cost monitoring efforts, such as the one which gave rise to the REMs, are valuable in generating new models since they allow data to be gathered from more missions over a greater period of time to complement data from higher performance instruments which fly more infrequently.

To address some of the modeling shortcomings, Brautigam et al. [7] produced a quasi-static model of outer-belt electrons based on an analysis of the data from the HEEF instrument of *CRRES*. *CRRES* was in a very similar orbit to *STRV* and the data from the on-board instruments were also very similar. The electron radiation belt during the *CRRES* mission was very dynamic. The mission highlight was the observation of the exceptional March 1991 event which led to the creation of a third radiation belt. Brautigam et al. established that the best way to describe the extreme variability of the outer zone was to create sub-models corresponding to states of the magnetosphere characterized by particular ranges of the Ap_{15} index. Ap_{15} is the 15-day average of the planetary Ap index, delayed by 1 day. Ap is itself derived from the planetary Kp index. This "quasi-static" model, known as CRRESELE, was an improvement to the de-facto standard electron radiation belt model, AE-8 [8], which is purely a long-term static average. CRRESELE also contains an "average" model.

In this paper, we present an analysis of data coming from a spacecraft in a very similar orbit to *CRRES*, but at solar minimum rather than the solar maximum conditions observed by *CRRES*. Comparisons are made with both CRRESELE and AE-8. Since CRRESELE is dependent on Ap_{15} as an activity indicator, the Ap_{15} records of the two periods (*CRRES* and *STRV*) are examined. Differences between the two periods are also established by examination of the long-term data set of >2 MeV electron fluxes at geostationary orbit as measured by detectors on the *GOES* spacecraft. This included examination of the relationship with the Ap_{15} record and comparisons with *STRV* REM data and CRRESELE.

II. Instrument and Spacecraft

REM registers, discriminates and counts the pulses of energy deposit (ΔE) generated by particle impacts on Si diode detectors [9]. The pulse-height discrimination is arranged to optimally respond to electrons, protons and heavy ions over 16 ΔE channels in each of the two independent detectors. Electrons in the MeV range deposit about the same energy as protons with E > 300 MeV. Therefore, these particles cannot be unambiguously distinguished from ΔE measurements alone. This can be solved by using detector stacks and active shielding, which complicates the system. In REM, the electron channels can be contaminated by protons, but the proton flux is independently measured to deduce the proton

contamination. Each detector uses a Si diode shielded by a spherical dome of 3 mm aluminum. One detector is shielded with an additional inner lining of ½ mm tantalum, which considerably lowers the penetration of MeV electrons. This we call the “p detector”; the other is the "e detector". The e detector on *STRV* is sensitive to protons with energies E >~30 MeV and to electrons with energies E >~1 MeV while the p detector responds to protons above 40 MeV. The energy deposit spectra are accumulated for typically 100 seconds and binned into 16 ΔE channels for each detector. The main aperture of the instrument is defined by a cone of 45°. On the *STRV* microsatellite, the surrounding shielding is not ideal and some very high-energy protons can penetrate from the sides. On *Mir*, the bulk of the station provides considerable rear shielding. Special efforts were made to determine the geometric and response factors of the REM detectors since these are crucial for deconvolution of the measured ΔE histograms to derive fluxes. The flight instruments were calibrated with protons and electrons at various energies. Monte-Carlo simulations were extensively applied, including realistic models of the mass distribution of the spacecraft.

STRV-1b was launched in June 1994 into a geostationary transfer orbit (GTO) which cuts through both inner (mainly proton) and outer (electron) radiation belts (~250 km perigee, 36000 km apogee, 7° inclination, 10½ hr. period). In late 1994 another model was fixed to the outside of the Russian space station *Mir*, in low Earth orbit (circular, ~400 km altitude, 52° inclination). The inclination of *Mir* means that at high latitudes it encounters the same geomagnetic field lines as *STRV* does at high altitude, so the data from the two instruments complement each other.

III. GTO Radiation Belt Measurements

The influence of solar-heliospheric events on the radiation belts is a strong feature of the REM observations[3]. The period covered by REM measurements corresponds to the declining phase of the 11-year solar activity cycle. Significant solar energetic particle events were absent and the solar wind (SW) arriving at the earth was characterized by recurrent fast SW streams [2].

Figure 1 summarizes the mission "dose" measurements, emphasizing the dynamism of the electron environment. "Dose" in this context is a "restricted dose", which is the energy deposited in the detector excluding the lowest ΔE channel. It should not be confused with total ionizing dose. The figure shows as a color scale the restricted dose rate (arbitrary units) as a function of time (in the mission) on the horizontal axis and geomagnetic L value (approximating geocentric radial distance) of the spacecraft location on the vertical axis. Because of the low inclination of the *STRV* orbit, little variation along field lines is seen and the data are assumed essentially omnidirectional and equatorial. The figure also shows the relative stability of the inner belt. The "injections" which characterize the outer belt are variable in nature. During spring 1995, several events occurred separated by the 27-day solar rotation period, indicating modulation by stable structures in the heliosphere. Some injection events result in long-lasting populations with slow inward radial transport and sometimes the slot region between the belts becomes very small.

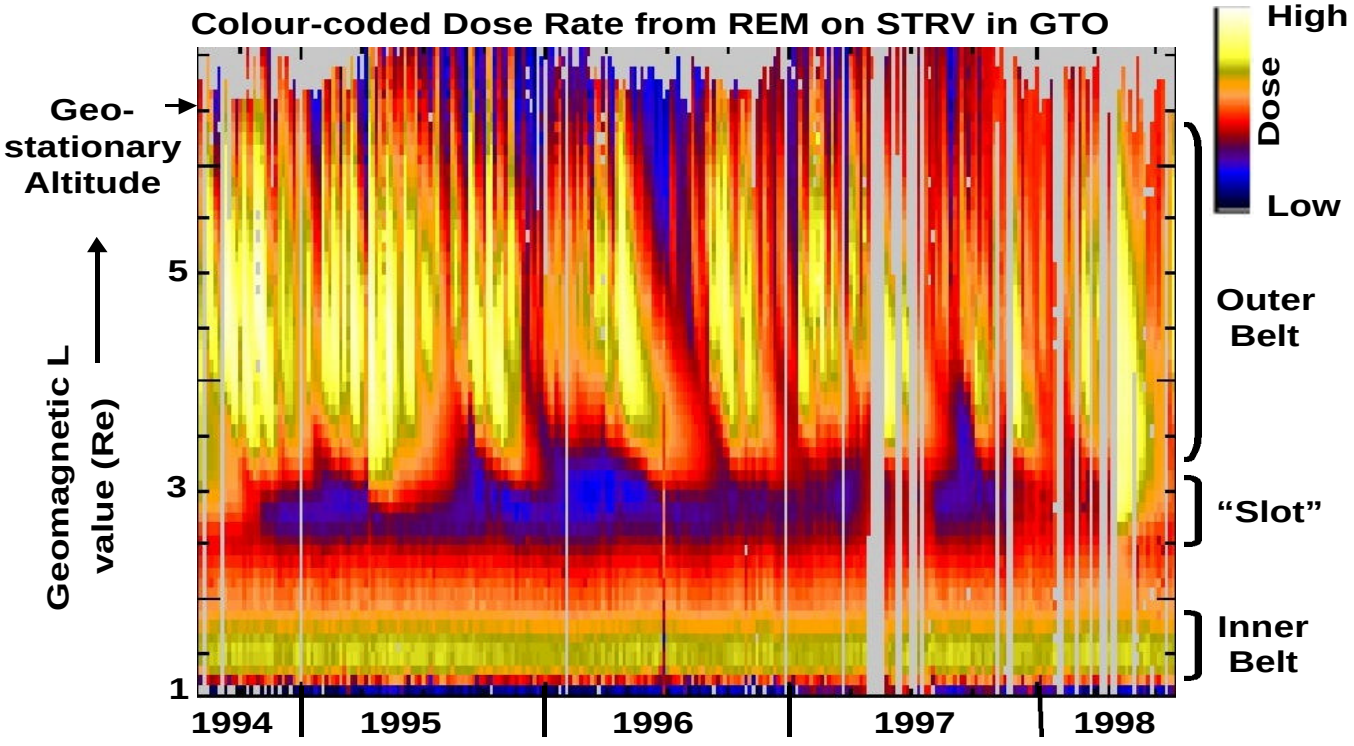

Figure 1: Summary of REM Observations: restricted dose (arbitrary units) as a function of time and L value.

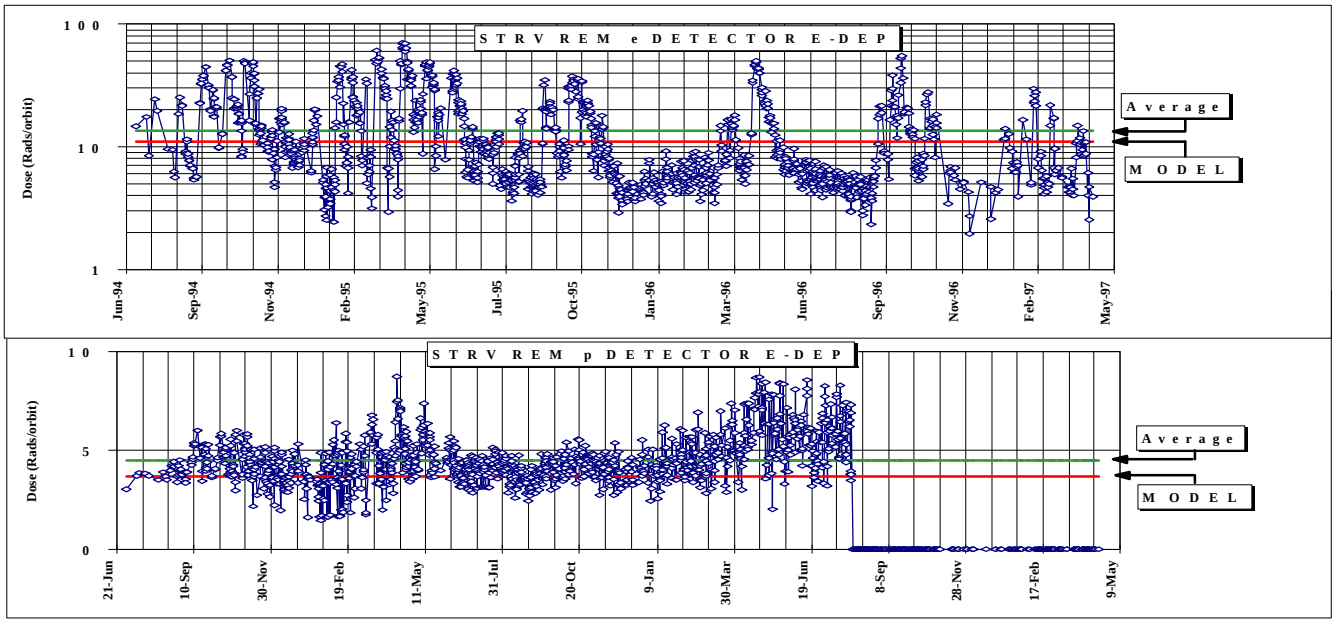

Figure 2 : Orbit total restricted dose for the two detectors. Also shown is the AE-8 + AP-8 sum expectation.

Figure 2 summarizes the orbit-sum restricted doses from the two detectors. Also shown are restricted doses predicted for this orbit by the static AE-8-MIN and AP-8-MIN models for the two detectors, when fluxes are folded with the detector response functions. P detector doses are not shown after July 1996 when the dead-time correction system for that detector became unusable. Note that the upper curve is plotted with a logarithmic dose scale while the lower one with a linear scale.

Both electron and proton models appear to underestimate dose, but only by a relatively small amount. Because of the dynamism, the electron environment is not well represented by the model for long periods, even though on average the agreement is reasonable. When compared with the model predictions of the "restricted dose" as a function of L-value, the average L-profile of the data are above the model over most of the outer zone as shown in Figure 3. This excess is due to the large storm events. The effect of the 0.75mm tantalum addition to the shield of the of the "p-detector" is also worth noting. The peak electron-belt doses can be seen to be down by a factor of about 30 as compared to the aluminium-only e-detector.

IV. Flux Results and Comparisons

With the instrument response functions which are themselves the result of extensive calibration and Monte-Carlo simulation, the count rates in the ΔE channels can be converted into fluxes in energy channels. This is more difficult for electrons than for protons but a reasonably good estimate can still be made near the shield penetration threshold energy (~1 MeV). One result of this is shown in Figure 4 where the average omnidirectional REM flux between 1 and 2.2 MeV over the period Nov 1994-Sept. 1996 is compared to the AE-8-MIN model for the same energy range.

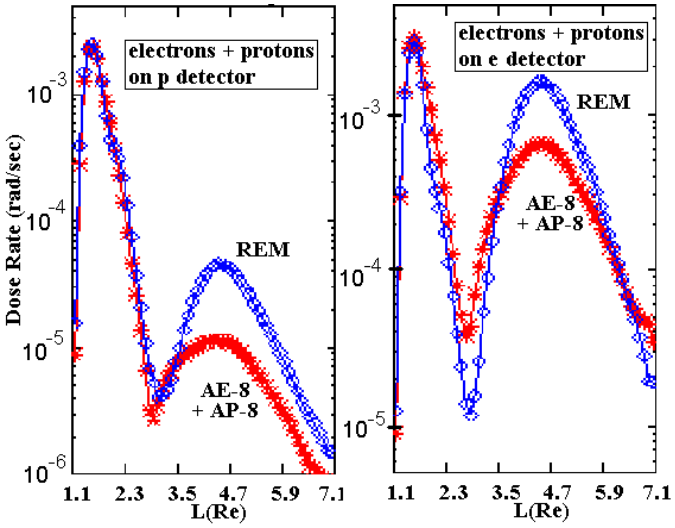

Figure 3: L-profile of REM dose-rate measurements compared to model-predicted "restricted dose".

Brautigam et al. [7] and Gussenhoven et al. [10] have shown that in many circumstances the *CRRES* measurements fall below the AE-8 model, especially at higher energies. At around 1MeV, at the peak of the outer belt, the CRRES average model fluxes were above AE-8 values. The REM results are consistent with those results. However, the CRRESELE model separated the *CRRES* environment into regimes characterized by Ap_{15} ranges, whose occurrence frequency may be different for different missions. Figure 5 shows the percentage of days of the *CRRES* and *STRV* missions with Ap_{15} in the various CRRESELE sub-model Ap_{15} ranges. It is clear from this that the *STRV* mission

coincided with generally lower Ap_{15} and one might therefore expect a milder environment.

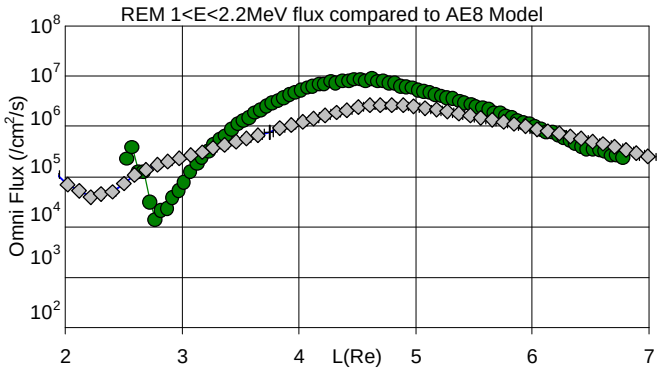

Figure 4: REM flux radial profile (circles) compared to equatorial AE-8 predictions (diamonds).

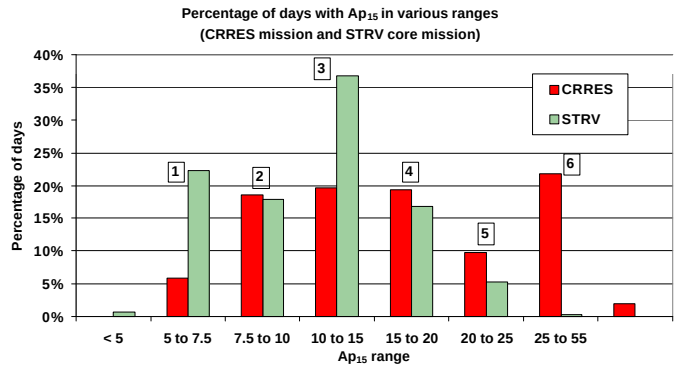

Figure 5: Ap_{15} occurrence percentage in each band corresponding to CRRESELE sub-models, which are numbered.

The REM flux data were used to construct sub-models in a similar way to *CRRES*, with each corresponding to the average flux during the various Ap_{15} ranges. These REM sub-models are shown in Figure 6. The variation between the sub-models for the 1<E<2.2 MeV model is similar to that seen in CRRESELE [10] for 0.95 MeV.

Having the Ap_{15} record for the *STRV* mission allows the CRRESELE model to be employed to "predict" an environment corresponding to the actual activity seen. Figure 7 shows the CRRESELE-derived flux profile for this period, produced by weighting the CRRESELE sub-models and averaging:

$$\bar{f} = \frac{\sum_{i=1}^{6} f_i . n_i}{\sum_{i=1}^{6} n_i} = \sum_{i=1}^{6} f_i . p_i$$

where i is the sub-model number, n_i represents the number of days Ap_{15} is in the range corresponding to the i^{th} model, f_i is the sub-model flux and p_i is the probability of an Ap_{15} values in the i^{th} range.

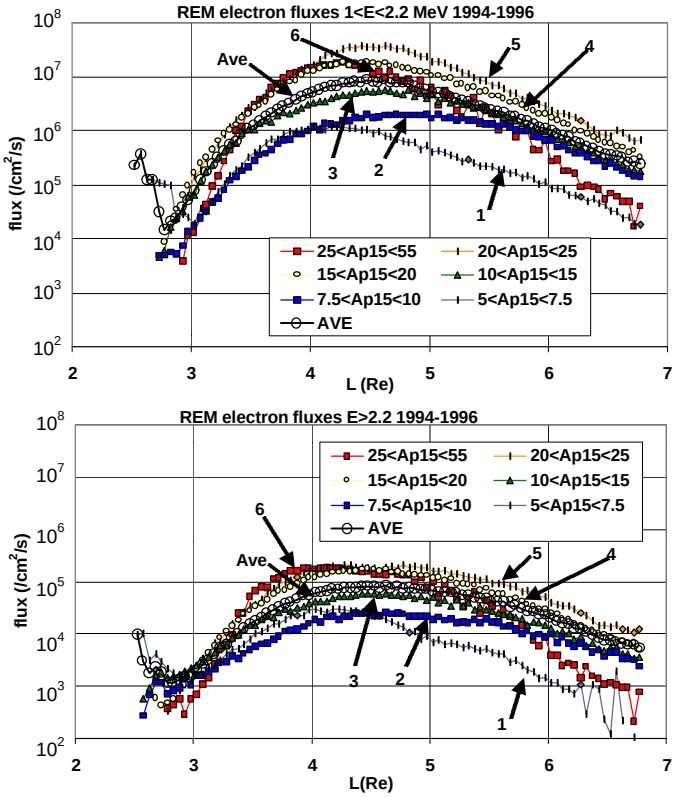

Figure 6: Sub-models derived from REM corresponding to various Ap_{15} activity ranges. The ranges are those used for CRRESELE. (a) 1-2.2MeV (b) >2.2MeV. The numbers help identify the sub-models and correspond to the ranges as shown in Figure 5.

This shows that even using the correct Ap_{15} history, the REM fluxes are not reproduced by the CRRESELE model; REM fluxes are still high.

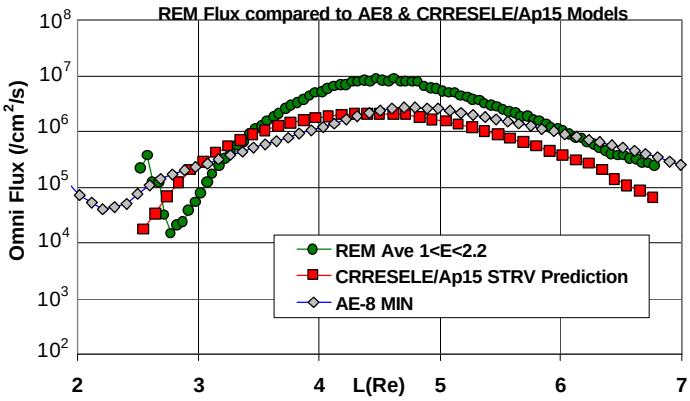

Figure 7: REM fluxes compared to a prediction made using CRRESELE sub-models and the actual Ap_{15} for the *STRV* period. Also shown is the AE-8-MIN prediction.

Since REM fluxes are apparently higher than expected, the uniqueness of the relationship between Ap_{15} and outer belt fluxes was examined. One of the few long-term data-sets available is the *GOES* >2 MeV omnidirectional electron flux

data set [11]. The daily average >2 MeV fluxes from *GOES* were binned according to Ap_{15} conditions for the two periods of interest (the *CRRES* mission and the *STRV* mission). The bins were again the Ap_{15} ranges used in the CRRESELE model. The result is shown in Figure 8.

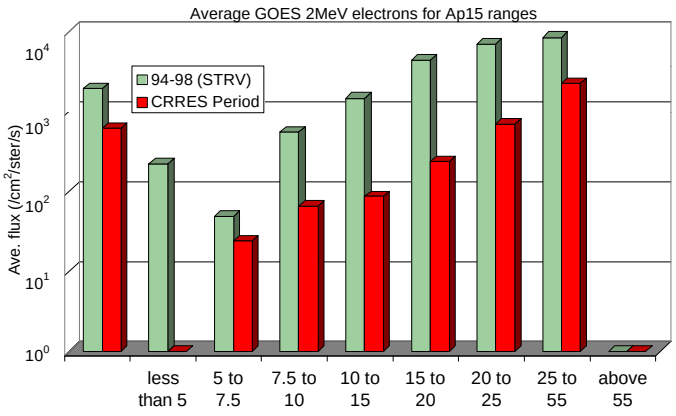

Figure 8: Average *GOES* >2 MeV electron fluxes for various Ap_{15} ranges during the *STRV* (upper) and *CRRES* (lower) periods.

The plot contains no information on the relative frequency of the conditions; it only represents the average flux when the conditions fall in a certain Ap_{15} band. Clearly, for any given Ap_{15} condition, the fluxes were much higher during the *STRV* mission than during the *CRRES* mission.

A further perspective on the differences between the *CRRES* and *STRV* periods is provided if one examines whether the rise in average flux in the *GOES* data is consistent with the differences between CRRESELE and REM-based models. To do this, the average electron fluxes from the CRRESELE and REM-based models for geostationary altitude were compared with AE-8 predictions and *GOES* measurements. This comparison is shown in Figure 9. The left-hand group corresponds to the *CRRES* period (AE-8 for >1 MeV; AE8 for >2.2 MeV; CRRESELE for >1 MeV; CRRESELE for >2.2 MeV; *GOES* >2 MeV) and the right-hand group to the *STRV* period (AE-8 for >1 MeV; AE-8 for >2.2 MeV; REM for >1MeV; REM for >2.2 MeV; *GOES* >2 MeV).

It can be seen that the differences between the *CRRES* period as indicated by CRRESELE and the *STRV* period as indicated by REM measurements are consistent with the increase in average flux seen by *GOES*.

V. Conclusions

The REMs on *STRV* and *Mir* are providing a wealth of interesting data. The orbit of *STRV* and the timing of the mission make this a good complement to the *CRRES* mission, allowing changes from solar maximum to solar minimum to be studied.

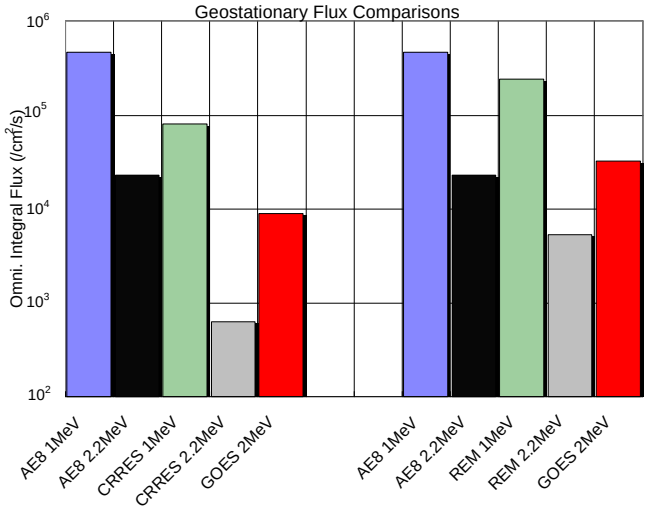

Figure 9: Various flux predictions and measurements made for the *CRRES* period (left group) and the *STRV* period (right group) for geostationary orbit.

Despite the simplicity of the REM instrument, data on electron fluxes can be derived and while at first sight these are unexpectedly high, it has been shown that the environment during the *STRV* period was more severe. Moreover, the relationship between Ap_{15} and electron belt fluxes is apparently not stable. The same Ap_{15} conditions at different parts of the solar cycle correspond to different fluxes. Further investigation of the use of Ap_{15} is needed.

Use of further long-term data-sets is necessary to establish the long-term behavior of correlations between energetic electron fluxes and indices. In addition, more missions in the *CRRES* and *STRV* type of orbits are necessary to map the belt.

The ultimate goal should be "model unification" but the modeling is apparently well short of that goal at present, at least for the outer belt. Among the critical questions posed by Gussenhoven et al. was: "*What is the solar cycle dependence of the particle distributions and can we produce solar cycle-dependent models?"*[10]. A lot more work is clearly needed before we can answer either of these.

Nevertheless, the proper modeling of the outer belt is of increasing importance in view of the effects it can have on spacecraft.

Acknowledgment

This work was supported by the Space Environments and Effects Major Axis of ESA's Technology Research Programme, under responsibility of ESA TOS-EMA.

REFERENCES

[1] P. Buhler, L. Desorgher, A. Zehnder and E. Daly, "Observation of radiation-belts and cosmic rays with REM", *Proceedings of ESA Workshop on Space Weather* ESA WPP-155 ISSN 1022-6656, November 1998.

[2] P. Bühler, L. Desorgher, A. Zehnder and E.J. Daly, "Radiation-belt energetic particle observations with REM", *Proceedings of the Spacecraft Charging Technology Conference*, November 1998, in press.

[3] P. Bühler, A. Johnstone, L. Desorgher, A. Zehnder, E.J. Daly and L. Adams, "The outer radiation belt during the 10 January, 1997 CME event"**,** *Geophys. Res. Letters* **25**, No. 15, Pages 2983-2986, August 1, 1998

[4] L. Desorgher, PhD Thesis, University of Bern, 1999.

[5] P. Bühler, L. Desorgher, A. Zehnder, E. Daly and L. Adams et al. "REM measurements aboard MIR during 1995", *Adv. Space Res.* 21, 1645, 1998.

[6] E. Daly, J. Lemaire, D. Heynderickx and D.J. Rodgers, "Problems with models of the radiation belts", *IEEE Transactions in Nucl. Sci.* NS-43, No. 2, April 1996.

[7] D.H. Brautigam, M.S. Gussenhoven and E.G. Mullen, "Quasi-static model of outer-zone electrons*", IEEE Trans. Nucl. Sci*, NS-39-6, 1797, 1992.

[8] J.I. Vette, "The AE-8 trapped electron model", NSSDC/WDC-A-R&S 91-24, 1991.

[9] P. Bühler, S. Ljungfelt, A. Mchedlishvili, N.Schlumpf, A. Zehnder, L. Adams, E. Daly and R. Nickson., "The radiation environment monitor", *Nucl. Instr. Methods*, A368, 825, 1995.

[10] M.S. Gussenhoven, E.G. Mullen and D.H. Brautigam, "Improved understanding of the Earth's radiation belts from the CRRES satellite", *IEEE Trans. Nucl. Sci.* NS-43, 2, April 1996.

[11] GOES data are available on www via the SPIDR system: http://spidr.ngdc.noaa.gov:8080/ production/html/GOES/index.html